6th International Conference on Advances in Experimental Structural Engineering
11th International Workshop on Advanced Smart Materials and Smart Structures Technology
August 1-2, 2015, University of Illinois, Urbana-Champaign, United States

Time-Dependent Considerations of I-35W St. Anthony Falls Bridge Including Long-Term Monitoring Applications

B.D. Hedegaard[1], C.E.W. French[2], C.K. Shield[3]

1 *Assistant Professor, Dept. of Civil and Environmental Engineering, University of Wisconsin – Madison, United States. E-mail: hedegaard@wisc.edu*
2 *CSE Distinguished Professor, Dept. of Civil, Environmental, and Geo- Engineering, University of Minnesota, Minneapolis, United States. E-mail: cfrench@umn.edu*
3 *CSE Distinguished Professor, Dept. of Civil, Environmental, and Geo- Engineering, University of Minnesota, Minneapolis, United States. E-mail: ckshield@umn.edu*

ABSTRACT
Structural health monitoring of in situ concrete structures is complicated by variations in the behavior of the structure due to ambient environmental conditions, transient loads, and time-dependent effects (e.g., creep and shrinkage of concrete, prestress losses). As a case study, the I-35W St. Anthony Falls Bridge, a post-tensioned concrete box girder bridge instrumented with over 500 sensors to monitor structural behavior, was studied over the first five years of operation. A data normalization scheme was developed to extract the time-dependent behavior of the bridge from long-term data, removing the instantaneous response due to thermal variations and adjusting the timescale with the Arrhenius equation to account for the temperature-dependent rate of time-dependent behavior. The resulting time-dependent behavior followed a line in log time, and served as the baseline for anomaly detection. Short-term and long-term checks were developed to identify anomalous, and thus potentially damage-related, changes in the time-dependent behavior. The efficacy of these checks was investigated by introducing perturbations into the monitoring data from the St. Anthony Falls Bridge, assumed to contain no damage, to simulate instantaneous bearing lockup and a slow degradation process through introduction of a two-year drift in the data. The proposed method succeeded in successfully identifying the perturbations while minimizing false positives.

KEYWORDS: *Structural monitoring, post-tensioned concrete, time-dependent behavior, temperature effects.*

1. INTRODUCTION

The goal of structural health monitoring is to provide tools for owners and engineers to evaluate the condition of an existing structure, identify problematic or damage-related behavior, and to use this knowledge to make informed decisions regarding the continued operation of the structure. Traditionally, this has been achieved through visual inspection; structural monitoring expands on this by offering quantifiable measurements, using a network of sensors, to more fully capture the in situ behavior of the structure.

In situ concrete structures are subject to changing temperature and humidity, time-dependent behavior, and transient loads, all of which impact the data collected by the monitoring system, but those changes may only be indicative of normal operation. Identifying damage that occurs suddenly, causing large and abrupt changes in sensor readings, may be simple if the damage-related changes are much greater than, or significantly different than the structure's natural behavior given changing environmental conditions. However, structural degradation may occur over the course of months or years and may be masked by natural variations in the collected data.

The I-35W St. Anthony Falls Bridge, a post-tensioned concrete box girder bridge in Minneapolis, Minnesota, was used as a case study for the development of a monitoring system that could be used to identify anomalous behavior (e.g., unanticipated instantaneous changes in response or long term degradation) in the presence of changing temperatures and time-dependent behavior. Methods for data normalization (i.e., the extraction of a particular behavior of interest from the measured data) and anomaly detection were developed through investigation of the behavior of the bridge over the first five years of operation in its undamaged state.

2. ST. ANTHONY FALLS BRIDGE

The St. Anthony Falls Bridge was constructed as two parallel post-tensioned box girder structures for northbound and southbound traffic. Each structure was designed as four spans, numbered as shown in Figure 2.1. The river span (Span 2) was constructed using precast segments cantilevered out from Piers 2 and 3 and connected at midspan with a cast-in-place closure pour. All other spans were cast-in-place using shored construction. Spans 1 through 3 were continuous with expansion joints located at Abutment 1 and Pier 4. Span 4 featured three-cell boxes in the northbound direction and two-cell boxes in the southbound direction, and was pinned at Pier 4 and built integrally with Abutment 5.

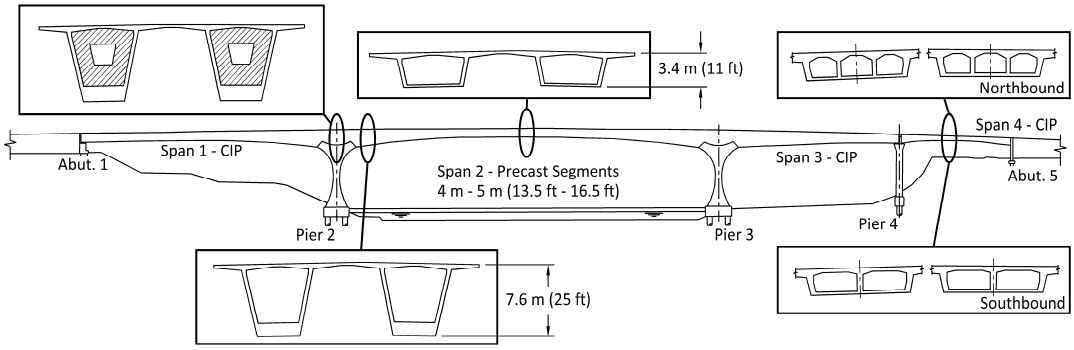

Figure 2.1 Elevation view of St. Anthony Falls Bridge (Hedegaard et al. 2013, © ASCE)

Over 500 sensors, including vibrating wire strain gauges (VWSGs), thermistors, long-gauge fiber optic sensors, accelerometers, and linear potentiometers (LPs), were installed in the St. Anthony Falls Bridge to investigate the structural behavior. Complete documentation of the instrumentation was provided by French et al. (2014). The scope of this paper is limited to the VWSG, thermistor, and LP data. These systems are briefly described below.

A total of 147 (112 in southbound, 35 in northbound) VWSGs were installed in the bridge superstructure at Locations 3, 4, 5, 6, 7, 8, 9, 14, and 15 in the southbound bridge, and Location 3, 5, 7, 8, 9, 14, and 15 in the northbound bridge, with location designations shown in Figure 2.2. All sections were instrumented with gauges in the top and bottom flanges to measure longitudinal curvature. Locations 3 and 7 of the southbound bridge were more heavily instrumented to investigate local deformations.

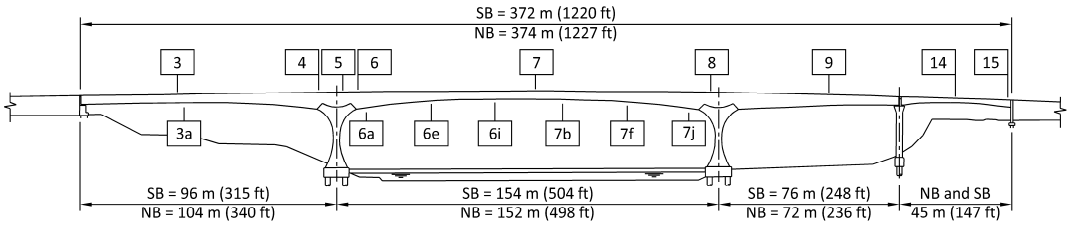

Figure 2.2 Instrumented location numbers (Hedegaard et al. 2013, © ASCE)

Though each VWSG contained an integral thermistor, 48 (42 in southbound, 6 in northbound) additional thermistors were installed in the superstructure. All individual thermistors were located at Location 7. Most were placed through the depth of the deck to capture the thermal gradient (i.e., temperature variations) caused primarily by solar radiation, with additional sets placed through the thickness of the webs and bottom flange.

Twelve (six in southbound, six in northbound) LPs measured the longitudinal displacements at the expansion joints at Abutment 1 and Pier 4. At Abutment 1, two LPs for each bridge were anchored from the superstructure web to the backwall of the abutment. At Pier 4, four LPs for each bridge were anchored to the top of Pier 4, with two attached to the Span 3 superstructure and two attached to the Span 4 superstructure. For clarity, sets of LPs are named according to the superstructure span to which they were anchored: Span 1, Span 3, or Span 4 LPs.

The collected data from each of the described sensors represented the structural response due to temperature, time-dependent effects such as creep and shrinkage, and other slowly developing phenomena. Readings,

collected each hour, were averaged over five minutes to remove any effects of transient live loads (expected to be negligible). Data are presented for the first five years of bridge operation, starting in September 2008.

3. DATA NORMALIZATION

Data normalization is the process of isolating a behavior of interest from other expected behavioral changes in measured data, and is an essential first step to structural monitoring in changing environments. If done properly, data normalization can enable the identification of anomalies of interest (e.g., bearing lock-up, structural deterioration, sensor malfunction), while minimizing the incidence of false positives (i.e., anomalies due to spurious readings).

Samples of the change in total strain and change in longitudinal displacement collected from the VWSGs and LPs, respectively, prior to data normalization are given in Figure 3.1. The data show strong seasonal trends due to annual temperature cycles, daily fluctuations from thermal gradients and daily temperature cycles, and a time-dependent trend due to creep and shrinkage. The time-dependent deformation of the bridge was chosen as the behavior of interest for data normalization, as this deformation progressed slowly and approximately monotonically, ideally allowing for identification of slowly developing degradation. For the remainder of this paper, only the longitudinal deflections measured by the LPs are examined, though the proposed method is applicable to both strain and deflection measurements.

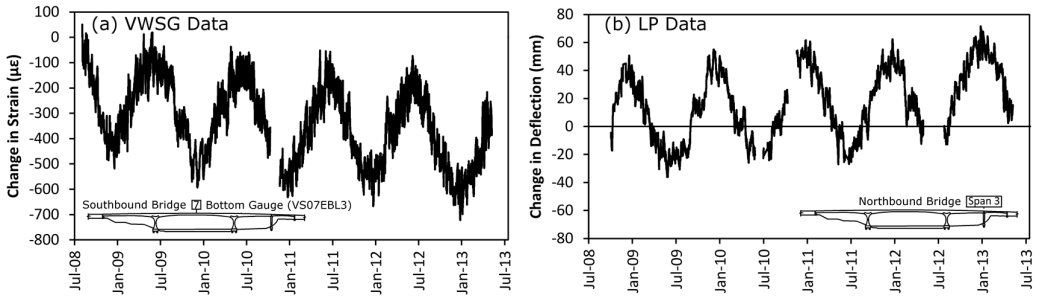

Figure 3.1 Sample change in total strain and change in longitudinal deflection readings over first five years

The temperature-dependent deformations were removed from the measured data by using linear regression, assuming an equation of the form

$$y = \alpha_1 \frac{\int T\,dA}{T_{ref} A} + \alpha_2 \frac{\int T^2\,dA}{T_{ref}^2 A} + \alpha_3 \frac{\int zT\,dA}{T_{ref} I_x / L_{ref}} + \alpha_4 \ln\left[1 + \left(\frac{t - t_0}{t_{ref}}\right)^{0.1}\right] + \alpha_5 + \delta \tag{3.1}$$

where y was the collected data from a sensor of interest, the α-coefficients were the fitting parameters for the linear regression, and δ was the residual, which aside from random noise may have also contained unexpected anomalies or systemic inaccuracies of the model.

The first term in Eq. 3.1 was related to longitudinal expansion of the bridge due to changes in the average temperature. The temperatures T used in this and the other terms of Eq. 3.1 were taken from the 42 thermistors at Location 7 of the southbound bridge, and area A referred to the cross-sectional area at Location 7. The reference temperature T_{ref} = 1.0°C non-dimensionalized the term. Inspection of the measured data revealed that the coefficient of thermal expansion of the structure varied linearly with temperature, as shown in Figure 3.2. The second term using the average squared temperature accounted for this observed phenomenon. The third term accounted for thermal gradients through the depth z of the cross section, which caused bending of the structure due to nonuniform expansion. This term was non-dimensionalized with the reference temperature, the gross moment of inertia I_x at Location 7, and a reference length L_{ref} = 1 m. The fourth term in Eq. 3.1 was the log-power curve, intended to approximate the time-dependent behavior from initial loading at t_0 (assumed to be July 25, 2008, corresponding to the placement of the midspan closure pour) to time of interest t, with t_{ref} = 1 day for non-dimensionalization. The objective of performing the linear regression was the isolation of the time-dependent behavior, and therefore the chosen time-dependent curve was required to compute the regression coefficients for the temperature terms. Five forms of the time-dependent regression curve were

investigated to find the α-coefficients in Eq. 3.1, but the determined coefficients were not sensitive to the selected time-dependent curve (French et al. 2014). Because only relative changes in deformation were known, the fitting coefficient α_5 was necessary for regression but did not have any physical basis.

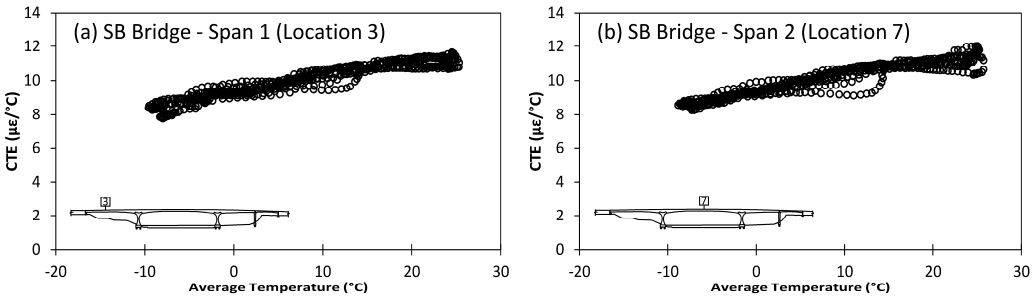

Figure 3.2 Variation of coefficient of thermal expansion (CTE) with bridge temperature

Using the α-coefficients from linear regression on data *y*, the time-dependent behavior *TD* plus the residual δ, which may contain unexpected anomalies in the data, was extracted using

$$TD + \delta = y - \alpha_1 \frac{\int T\,dA}{T_{ref} A} - \alpha_2 \frac{\int T^2\,dA}{T_{ref}^2 A} - \alpha_3 \frac{\int zT\,dA}{T_{ref} I_x / L_{ref}} - \alpha_5 \tag{3.2}$$

The time-dependent longitudinal deflections plus residual from the LPs are plotted in Figure 3.3. The linear regression procedure appeared to account for the instantaneous deformations caused by temperature changes. However, removal of the instantaneous thermal effects revealed that the rate of the time-dependent deformation was temperature dependent; creep and shrinkage slowed during the winter and accelerated during the summer.

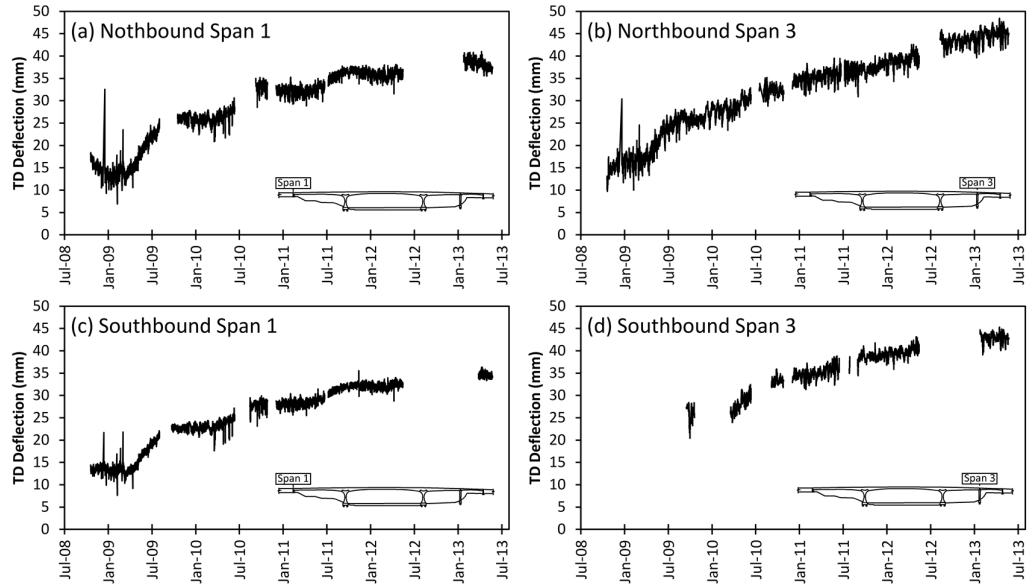

Figure 3.3 Time-dependent longitudinal deflection extracted from LP data for first five years

The final step of data normalization was to define an "adjusted time" t_{adj} accounting for the temperature-dependent rates of creep and shrinkage, computed using the Arrhenius equation:

$$t_{adj} = \int_{t_0}^{t} e^{\left[\frac{Q}{R}\left(\frac{1}{T_0} - \frac{1}{T(t')}\right)\right]} dt' \tag{3.3}$$

where the start time for integration t_0 was July 25, 2008 when the midspan closure pour was placed, t was the unadjusted time of interest, Q/R was the activation energy constant, T_0 was the reference temperature equal to 293 K (20°C), $T(t')$ was the temperature history in Kelvin, and integration time t' was specified in days. The value of Q/R represented an aggregate activation energy for all time-dependent processes, as creep and shrinkage could not be separated in the measured data, and was set equal to 7360 K according to the expression for activation energy of basic creep given by Bažant and Baweja (1995) using nominal material properties of the St. Anthony Falls Bridge superstructure concrete mix. The temperature history $T(t')$ was taken as the average temperature computed over the cross section at Location 7 of the southbound bridge. This adjusted time represented the time under constant temperature conditions at T_0 that would return equal time-dependent deformations as those measured under varying temperature conditions $T(t')$.

The same adjusted time was assigned to all sensors, regardless of loading and temperature history at the location of the sensor. This approximation was adopted to facilitate comparison of data from sensors installed at different locations across the bridge. Parts of the bridge were stressed prior to July 25, 2008 in the construction sequence, and assigning a different integration start time individually for each sensor would have been justified. To further complicate matters, the rate of time-dependent behavior at any given location depended on the constitutive equation, a function of the temperature at that location, and also strain compatibility, a function of the strain rates and temperatures throughout the entire structure. The proposed expression did not account for these phenomena separately, but still reasonably captured the observed temperature-dependent rate of time-dependent behavior.

The extracted time-dependent longitudinal deflections, plotted in Figure 3.4 with respect to the adjusted time (log scale), followed a line with respect to the logarithm of adjusted time. This trend was consistent with the predicted shape of the creep and shrinkage curves according to the B3 model (Bažant and Baweja 1995), which prescribes a logarithmic creep function, and also the GL2000 model (Gardner and Lockman 2001), which approximates a logarithmic function for timescales up to thousands of years. For structures with large volume-to-surface ratio, such as the St. Anthony Falls Bridge, the 1990 CEB-FIP Model Code provisions also provide a curve that nearly follows a line in log time over the duration of the collected data, but unlike the aforementioned models approaches an asymptotic value over a timeframe on the order of 100 years. Creep and shrinkage provisions from AASHTO (2008) and ACI-209 (1992) approach asymptotic values within a timeframe of three to five years, and thus are not consistent with the extracted time-dependent behavior in Figure 3.4. The AASHTO and ACI-209 provisions account for the volume-to-surface ratio of the structure by scaling the ultimate creep and shrinkage strains but not altering the rate at which these asymptotic limits are approached, a method unique to these two provisions among the discussed models and at odds with the observed behavior.

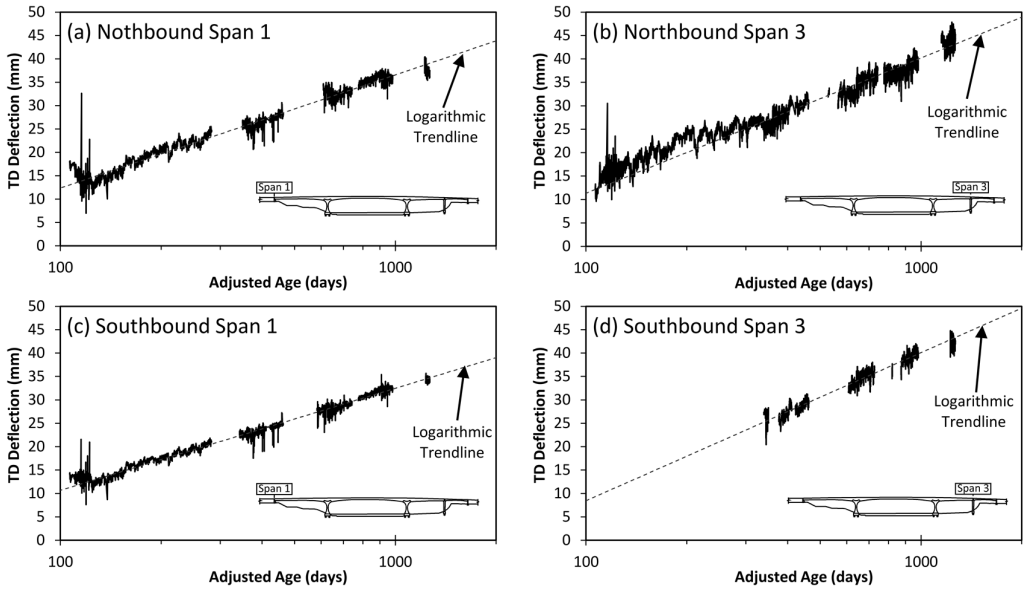

Figure 3.4 Time-dependent longitudinal deflections plotted with respect to Arrhenius adjusted time

4. ANOMALY DETECTION

The proposed data normalization technique offered a promising baseline for identifying anomalies in strain and deflection readings that might be indicative of immediate issues or slowly developing issues. For example, changes in the time-dependent longitudinal displacement might be indicative of bearing lockup, unexpected acceleration of creep (possibly due to reduction of stiffness in the superstructure), unexpected deceleration in the rate of creep (possibly due to loss of post-tensioning force), or sensor failure. To facilitate anomaly detection, two separate checks were developed: the short-term check for investigating anomalies developing over the course of a month or less, and the long-term check for anomalies developing over the course of several years. The proposed methods could only alert maintenance personnel about the presence of an anomaly, and could neither locate the problem nor diagnose the cause.

The short-term check was based on a Bayesian statistical framework, whereby an initial estimate, or prior distribution, of the time-dependent behavior was updated using the measured data from the monitoring system, arriving at the posterior distribution. The prior distribution was assumed to be Gaussian, and was computed separately for six different time-dependent provisions: ACI-209 (1992), B3 (Bažant and Baweja 1995), both 1978 and 1990 CEB-FIP Model Codes, GL2000 (Gardner and Lockman 2001), and AASHTO (2010) modified to include the ACI-209 concrete aging provisions. The mean of the prior distribution was computed using time-dependent finite element models of the St. Anthony Falls Bridge that included the full construction sequence, post-tensioning losses, and a rate-type creep formulation (French et al. 2014). The coefficient of variation of the prior distribution varied depending on the selected time-dependent model, ranging from 25% to 33%, according to studies by Gardner (2004), Bažant and Li (2008), and Keitel and Dimmig-Osburg (2010). These large coefficients of variation led to wide credible bounds on the initial prediction, which were not useful for identifying anomalous data.

The time-dependent behavior extracted from the monitoring data was divided into a training set, consisting of all past data except the most recent 1000 hourly readings (approximately 42 days), and a test set, containing only the most recent 1000 hourly readings. The training set was used to update the prior distribution via Bayesian regression, and the resulting posterior distribution was compared to the test set. If enough readings in the test set were outside the credible bounds of the posterior distribution such that the probability of such an event was sufficiently low, the test set was categorized as an anomaly. Using the Bayesian statistical framework, the credible bounds of the posterior distribution were reduced by an order of magnitude compared to the bounds from the prior distribution, as shown in Figure 4.1 (95% credible bounds plotted).

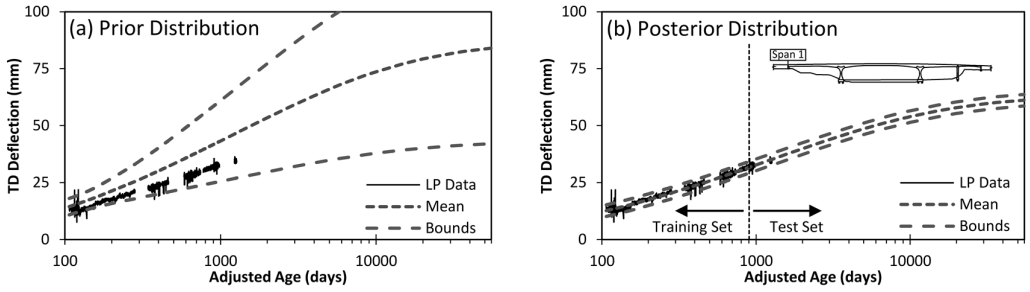

Figure 4.1 Prior and posterior distributions for short-term anomaly detection check performed on time-dependent behavior from southbound Span 1 LPs, assuming 1990 CEB-FIP Model Code provisions

While using Bayesian regression to predict the bounds over a test set of 1000 hourly readings was reliable, the efficacy of this method for long-term anomaly detection (on the order of several years) was strongly dependent on the time-dependent provisions chosen to build the prior distribution. To avoid this complication, the Bayesian framework was not used for long-term anomaly detection. Instead, the rates of time-dependent strains or longitudinal deflections were calculated and compared to bounds chosen to minimize false positives when verified on the extracted rates from the measured data, assumed to contain no damage-related behavior.

To compute long-term creep and shrinkage rates, a log-power curve was fit to windows of two-year duration of extracted time-dependent data:

$$TD = \beta_1 \ln\left[1 + \left(\frac{(t - t_0)_{adj}}{t_{ref}}\right)^{0.1}\right] + \beta_2 + \delta \tag{4.1}$$

where *TD* was the extracted time-dependent behavior, $(t - t_0)_{adj}$ was the adjusted time, t_{ref} = 1 day, and δ was the residual. The β-coefficients were computed using weighted linear regression, such that the window was divided into 20 bins of equal adjusted age, with each bin given equal weight in the regression to prevent bias towards clusters of readings during the winter, which all had similar adjusted time and time-dependent readings. Because the computed rate of time-dependent behavior, or equivalently the derivative of TD with respect to $(t - t_0)_{adj}$, at any time in a given window was proportional to the fitting constant β_1, only the rate computed at the beginning of each window was used for anomaly detection.

The rates computed from the first year of windows (containing the first three years of data) were used as the training set, to which a steadily decreasing power law was fit:

$$\frac{\partial(TD)}{\partial(t - t_0)_{adj}} = \gamma\left(\frac{(t - t_0)_{adj}}{t_{ref}}\right)^{-0.9} + \delta \tag{4.2}$$

where γ was computed using weighted linear regression on 20 bins of equal adjusted time (taken at the beginning of the window), with each bin given equal weight. The fitted power law was extrapolated to the test set containing all windows past the training set, and this extrapolation was assumed to be the mean of the expected time-dependent rates. Windows with rates outside the chosen bounds were classified as anomalous. An example of the computed time-dependent rates, resulting fit, and extrapolation to the test set (i.e., all data beyond the training set) is given in Figure 4.2.

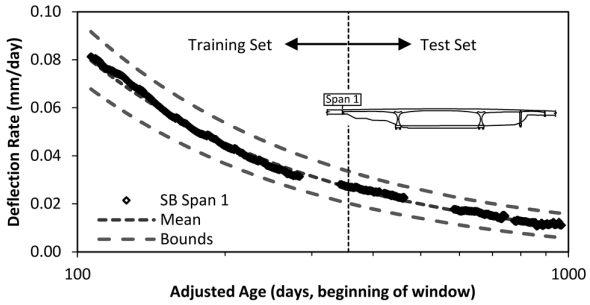

Figure 4.2 Rate of time-dependent longitudinal deflection from southbound Span 1 LPs

Because anomalous data are not necessarily indicative of structural degradation, but may be false positives, the anomaly detection routines were tested on the first five years of monitoring data from the St. Anthony Falls Bridge for which no degradation was present (and thus any anomaly could be categorized as a false positive) and on the same data with artificially introduced perturbations (which if properly detected could be categorized as "damage"). For the short-term check, predictions using the 1990 CEB-FIP Model Code, B3, and GL2000 provisions were able to detect artificially induced jumps in the LP data of 6 mm (0.25 in.). For comparison, horizontal deflections at the expansion joints due to annual temperatures cycles were on the order of 80 mm (3.1 in.), and time-dependent horizontal deflections were on the order of 30 mm (1.2 in.) over the five years of monitoring. All investigated models were able to detect perturbations mimicking bearing lockup, whereby the deflections due to daily temperature changes were suddenly subtracted from the data. The 1990 CEB-FIP Model Code, B3, and GL2000 provisions minimized the incidence of false positives for the St. Anthony Falls Bridge data as compared to the ACI-209, AASHTO, and 1978 CEB-FIP Model Code provisions. The long-term check was able to detect perturbations as subtle as an artificially induced drift of 6 mm (0.25 in.) over a duration of two years (approximately 0.008 mm/day).

5. SUMMARY AND CONCLUSIONS

The St. Anthony Falls Bridge was used as a case study for examining long-term monitoring applications in the

presence of changing ambient conditions. Data collected from structural monitoring systems contain information from many inputs, including temperature, ambient humidity, time, external loads, and possibly structural degradation. Data normalization is the process of extracting the behavior of interest from the data. Anomaly detection is the diagnosis of the extracted behavior as unexpected or anomalous.

In the case of the St. Anthony Falls Bridge, the static, long-term data was primarily driven by the structural response to temperature changes and time-dependent behavior. For data normalization, the time-dependent behavior due to creep and shrinkage of the bridge was extracted from the measured data using linear regression. The temperature-dependent behavior was approximated as a summation of three terms: uniform expansion due to average temperature changes, uniform expansion associated with the linear change in coefficient of thermal expansion, and bending associated with thermal gradients. When subtracted from the measured data, the rate of the resulting time-dependent behavior varied with bridge temperature, such that time-dependent effects decelerated in the winter and accelerated in the summer. After applying an adjusted time scale using the Arrhenius equation, the extracted time-dependent behavior followed a linear trend in log time.

The normalized data was used as the basis of an anomaly detection routine intended to identify short-term anomalies developing over at most several weeks and long-term anomalies developing over several years. The goals of this routine were to minimize false positives, tested using the St. Anthony Falls Bridge data which was presumed to contain no damage-related behavior, and to ensure the detection of anomalous signals, tested by introducing perturbations into the monitoring data. The short-term check used Bayesian regression to compute credible bounds for time-dependent behavior over the most recent 1000 hourly readings, flagging the set as anomalous if enough readings in the test set fell outside the credible bounds. The long-term check examined the rates of the time-dependent behavior over two-year windows. These rates were assumed to decrease with increasing adjusted time, and thus were modeled using a power law. Together, these two checks successfully identified artificially introduced anomalies of instantaneous jumps, bearing lockup, and slow drift in the longitudinal displacement data at the expansion joints.

AKCNOWLEDGEMENT
The authors would like to acknowledge the support of the Minnesota Department of Transportation. Numerical computations were performed using resources provided by the University of Minnesota Supercomputing Institute. The opinions expressed herein represent those of the authors and not necessarily those of the sponsors.

REFERENCES

1. ACI Committee 209 (1992). ACI-209R-92 Prediction of Creep, Shrinkage, and Temperature Effects in Concrete Structures, American Concrete Institute, Detroit, MI.
2. American Association of State Highway and Transportation Officials (2010). LRFD Bridge Design Specifications, Fifth Edition, AASHTO, Washington, DC.
3. Bažant, Z.P., and Baweja, S. (1995). Creep and Shrinkage Prediction Model for Analysis and Design of Concrete Structures: Model B3. *Materials and Structures*. **28:6**, 357-365.
4. Bažant, Z.P., and Li, G.-H. (2008). Unbiased Statistical Comparison of Creep and Shrinkage Prediction Models. *ACI Materials Journal*. **105:6**, 610-621.
5. Comité Euro-Internationale du Béton and Fédération Internationale de la Précontrainte (1978). 1978 CEB-FIP Model Code, Thomas Telford Services Ltd., London, UK.
6. Comité Euro-Internationale du Béton and Fédération Internationale de la Précontrainte (1990). 1990 CEB-FIP Model Code, Thomas Telford Services Ltd., London, UK.
7. French, C.E.W., Shield, C.K., and Hedegaard, B.D. (2014). Modeling and Monitoring the Long-Term Behavior of Post-Tensioned Concrete Bridges, Report MN/RC 2014-39, Minnesota Dept. of Transportation, St. Paul.
8. Gardner, N.J., and Lockman, M.J. (2001). Design Provisions for Drying Shrinkage and Creep of Normal-Strength Concrete. *ACI Materials Journal*. **98:2**, 159-167.
9. Gardner, N.J. (2004). Comparison of Prediction Provisions for Drying Shrinkage and Creep of Normal-Strength Concretes. *Canadian Journal of Civil Engineering*. **31:5**, 767-775.
10. Hedegaard, B.D., French, C.E.W., Shield, C.K., Stolarski, H.K., and Jilk, B.J. (2013). Instrumentation and Modeling of I-35W St. Anthony Falls Bridge. *Journal of Bridge Engineering*. **18:6**, 476-485.
11. Keitel, H., and Dimmig-Osburg, A. (2010). Uncertainty and Sensitivity Analysis of Creep Models for Uncorrelated and Correlated Input Parameters. *Engineering Structures*. **32:11**, 3758-3767.